International Conference on Environment 2015 (ICENV 2015)
Instruction to Authors

APPLICATION OF $CuFe_2O_4$ FOR PHOTOCATALYTIC FENTON TREATMENT OF GLYCEROL SOLUTION

ZI YING KONG[1], CHIN KUI CHENG[1,2], MAKSUDUR R. KHAN[1]
[1]Faculty of Chemical & Natural Resources Engineering
[2]Rare Earth Research Centre
Universiti Malaysia Pahang, Lebuhraya Tun Razak 26300 Gambang, Pahang
Malaysia
michellekzy89@gmail.com

ABSTRACT

This study reports on the glycerol decomposition using photocatalytic fenton technique. Visible light-responsive $CuFe_2O_4$ photocatalyst was synthesized using sol-gel method employing Cu:Fe ratio of 1:2 by mol. In the presence of xenon lamp (250 W), the performance of photocatalytic fenton degradation of different concentrations of glycerol aqueous solution (27.36, 41.05, 54.73 and 68.41 mM), different concentrations of hydrogen peroxide (163.9, 327.8, 491.7, 655.6 and 819.5 mM) and different photocatalyst loadings (0.1, 1.0, 2.0 and 5.0 g/L) were studied. The results obtained show that a minimal amount of photocatalyst loadings (0.1 g/L) was needed to initiate the photocatalytic fenton reaction. When the concentration of glycerol was increased, the degradation of glycerol diminished; however increasing the concentration of H_2O_2 has increased the glycerol degradation. The degradation for initial glycerol concentration of 27.36 mM was 60.0% while at 67.41 mM glycerol concentration, the degradation attained 27.0%. Besides that, adding 819.5 mM H_2O_2 showed 30% degradation while adding 163.9 mM H_2O_2 only showed 5% degradation. Full factorial analysis was introduced to screen the factors in the photocatalytic fenton degradation of glycerol. The screening exercise indicates that the best conditions were 27.41 mM glycerol concentration, 819.5 mM H_2O_2 concentration and 5.0g/L photocatalyst loadings in the experiment of four hours.

Keywords: Copper ferrite; Fenton; Glycerol; Photocatalytic

INTRODUCTION

Fossil fuels have been the main sources of the global demand energy over the years [1]. However, these fossil fuels are fast depleting and may eventually insufficient to meet the world's growing energy needs [2-3]. Hence, alternative fuels such as biogas, biofuel and biodiesel have been widely investigated, experimentally. Biodiesel is a fuel produced via trans-esterification of vegetable oils or animal fats with alcohol such as methanol [4]. In fact, it is a primary by-product during biodiesel production [5]. According to Yang et al. [6], production of biodiesel will generate 10% (w/w) glycerol. Biodiesel production is predicted to increase in the future; consequently, large amount of glycerol is expected. The glycerol produced from biodiesel still contains impurities such as methanol, free fatty acids (soaps), unreacted catalyast and water [7-8]. In addition, it also contains various kinds of elements such as calcium, magnesium, phosphorous, or sulfur [9]. To minimize impacts to the environment, degradation of glycerol is vital. Due to the complexity of crude glycerol composition, a lab-prepared aqueous glycerol was employed as the model compound for the current study.

Several treatment methods such as physico-chemical, electrochemical, coupled chemical and electrochemical, advanced oxidation, biological, integrated chemical and biological,

integrated chemical, electrochemical and biological, and biological have been investigated to treat the wastewater [5,10]. These methods have been shown to achieve different levels of efficiencies for the treatment of the biodiesel waste water [5]. However, due to the number of unit operations involved in these treatment processes, it is capital intensive to efficiently treat the waste water.

One effective way to reduce the number of unit operations involve in the waste water treatment process and hence reduce cost is the photocatalysis. Photocatalysis is a photo reduction process using photocatalyst. In this study, a photocatalyst was employed for the degradation of glycerol. Past research works on glycerol degradation were mostly eomploying TiO_2-based photocatalyst, i.e. Pt/TiO_2 [11], Pt loaded N-doped TiO_2 [12], cobalt doped TiO_2 [13], NiO_x/TiO_2 [14] and others. However, these TiO_2 based photocatalysts are hampered by two serious disadvantages. The first is the agglomeration of ultrafine powders resulting in an adverse effect on catalyst performance [15]. The second is the wide band gap of TiO_2 (> 3.1 eV) which restricts its photocatalytic applications to the UV range (200 to 400 nm). Unfortunately, UV spectrum accounts for merely 4% of the solar energy spectrum, and consequently results in low photo-electronic transition efficiency [16-17]. Thus, it is highly advantageous to develop a new breed of photocatalysts that can function under visible light illumination.

In this study, $CuFe_2O_4$ was prepared using sol gel method as it is a superior method compared to solid-solid method and co-precipitation method [18]. Moreover, $CuFe_2O_4$ photocatalyst was employed in the fenton treatment of glycerol through different concentrations of glycerol (27.36, 41.05, 54.73 and 68.41 mM) and different catalyst loading (0.1, 1.0, 2.0 and 5.0 g/L) as well as different concentrations of hydrogen peroxide (H_2O_2) (163.9, 327.8, 491.7, 655.6 and 819.5 mM).

EXPERIMENTAL

Chemical and Materials. Copper (II) Nitrate Trihydrate, Iron (III) Nitrate nonahydrate, citric acid and glycerol were purchased from Sigma Aldrich. Hydrogen peroxide (30%) was procured from Merck while acetonitrile (HPLC grade) was sourced from Fischer Chemical. All the chemicals were used as-received.

$CuFe_2O_4$ Photocatalyst Synthesis. The $CuFe_2O_4$ photocatalyst was prepared using the sol-gel method. Accurately-weighed 0.005 mol $Cu(NO_3)_2 \cdot 3H_2O$ and 0.01 mol $Fe(NO_3)_3 \cdot 9H_2O$ were co-dissolved in 50 ml distilled water. The mixed solution was subsequently added into 100 ml of 0.3 M citric acid solution. A transparent mixed-sol was produced as a result. During the mixing, the temperature of solution was controlled at 80°C until a transparent and viscous gel was obtained. The as-obtained gel was subsequently transferred into an oven and dried at 140°C for 3 h. The as-prepared catalyst was then air-calcined at 850°C for 3 h at a ramping rate of 10°C min^{-1}. The calcined catalyst was then ground and stored in the vials for catalyst characterization and photocatalytic fenton study.

Photocatalytic Activity. For the reaction study, around 200 ml of slurry media was irradiated with visible light source. Pre-determined photocatalyst loading was dispersed in 200 ml of different concentrations of glycerol and H_2O_2 solution mixture in the photoreactor. Subsequently, the mixture was stirred rigorously for 30 min (without light source) to attain equilibrium, followed by exposure to a light source for reaction initiation. Approximately 5 ml of liquid

sample was collected every 1 h for analysis. All the experiments were repeated twice. Overall, three types of effects have been investigated, *viz*. (i) the effects of photocatalyst loadings (0.1, 1.0, 2.0 and 5.0 g/L) on glycerol degradation, in a reaction media of 200 mL of 68.41 mM glycerol solution and 819.5 mM of H_2O_2, (ii) the effects of initial concentration of glycerol (27.36, 41.05, 54.73 and 68.41 mM) on glycerol degradation, in a reaction media of 0.1 g/L $CuFe_2O_4$ and 819.5 mM of H_2O_2 and also (iii) the effects of H_2O_2 concentration (163.9, 327.8, 491.7, 655.6 and 819.5 mM) on glycerol degradation, conducted in 200 mL of 68.41 mM glycerol solution and 0.1 g/L $CuFe_2O_4$.

Sample Analysis. All the collected samples were centrifuged before subjected to HPLC analysis. Quantitative sample analysis was performed using Agilent 1200 Series HPLC equipped with refractive index (RI) detector. The column used in this study was Agilent Zorbax Carbohydrate 5μm column (inner diameter of 4.6 and length of 250 mm) with the flow rate of 1.0 mL/min and injection volume of 10 μm. The mobile phase used throughout the HPLC analysis was acetonitrile (ACN) diluted with ultrapure water in a ratio of 7:3. Prior to the HPLC analysis, the mobile phase was filtered using a nylon membrane with pore size of 0.2 μm, then degassed using ultrasonic bath at room temperature for 30 min.

Factorial Experimental Design. Experimental design was carried out using Design Expert software (version 7.0) following the methodology of full two level factorial design. The variables and levels are summarized in Table 1. The analysis of variance (ANOVA) was conducted using Design Expert software (version 7.0) to analyze and check the significance of the fitted models.

Table 1: Factors and their designated low and high value

Factor	Units	Low Value (-1)	High Value (+1)
A: Time	h	1	4
B: Glycerol concentration	mM	27.36	68.4
C: H_2O_2 concentration	mM	163.9	819.5
D: $CuFe_2O_4$	g/L	0.1	5

RESULTS AND DISCUSSION

Effects of Photocatalyst Loadings. Experiments for determination of the effects of initial catalyst loading were carried out at 68.4 mM of glycerol and 819.5 mM of H_2O_2 and the results are as shown in Figure 1. The blank run (without catalyst) indicates that photolysis reaction occurred and achieved glycerol degradation of 17.7% after 4 h of reaction. In the presence of $CuFe_2O_4$ photocatalyst, the onset of photocatalytic fenton reaction has increased the degradation of glycerol substantially, i.e. at 0.1 g/L of photocatalyst loading, the degradation of glycerol can attain 27.0% and peaked at almost 40.0% of glycerol degradation when 5.0 g/L of $CuFe_2O_4$ photocatalyst loading was employed. By increasing the photocatalyst loadings from 0.1 to 5.0 g/L, the number of active sites would have increased in tandem, consequently, the glycerol degradation also increased. Nevertheless, if excessive amount of catalyst is used, it may have block the penetration of light source and consequently, it lowers the glycerol decomposition rate.

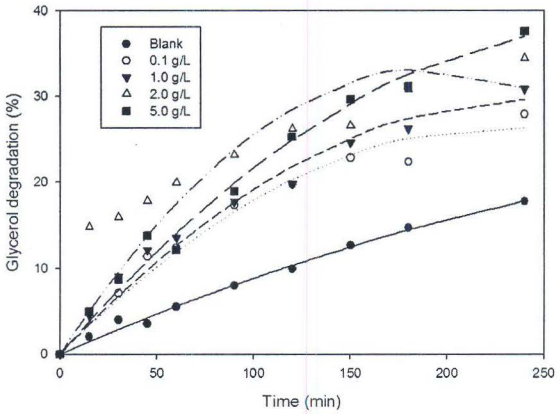

Figure 1: Glycerol degradation at different photocatalyst loadings

Effects of Initial Concentration of Glycerol. In order to study the effects of initial glycerol concentration on glycerol decomposition, the initial concentration was varied from 27.36 mM to 68.41 mM in the presence of 0.1 g/L of $CuFe_2O_4$ and 819.5 mM H_2O_2 as shown in Figure 2. By increasing the initial glycerol concentration, the glycerol degradation has decreased. Indeed, at 27.36 mM initial glycerol concentration, degradation was nearly 60.0%. In contrast, when the initial glycerol concentration was 68.41 mM, the degradation has dropped to attain about 30.0% only.

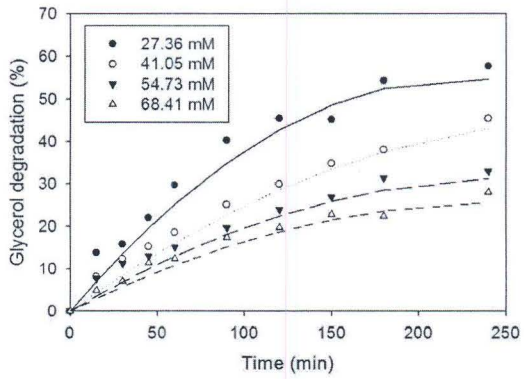

Figure 2: Glycerol degradation at different initial glycerol concentration

Effects of Initial Concentration of Hydrogen Peroxide. Initial H_2O_2 concentration would also affect glycerol decomposition at constant 68.4 mM glycerol concentration and loading of 0.1 g/L $CuFe_2O_4$ as shown in Figure 3. The increase in H_2O_2 concentration would produce more $^{\bullet}OH$ radical; hence increase the degradation of glycerol. At 163.9 mM of initial H_2O_2 concentration, the degradation rate was 5%. By increasing the initial H_2O_2 concentration from 163.9 mM to 819.5 mM, the degradation was also increasing from 5.0% to 25.0%.

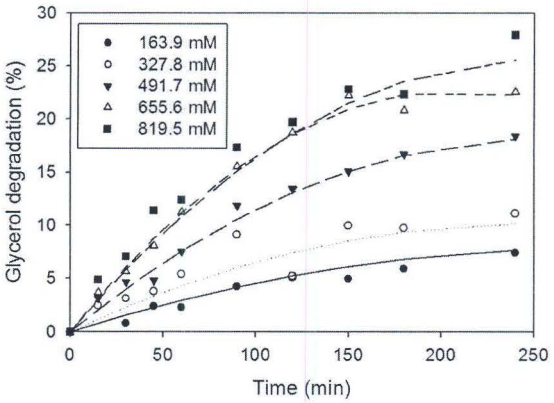

Figure 3: Glycerol degradation at different initial hydrogen peroxide

Factorial Analysis on Glycerol Degradation. Figure 4 shows the main effects of factors in Pareto chart by conferring t-value limit. According to the Pareto chart, effects above the t-value limit are considered 99% confidence level. It can be seen that H_2O_2 concentration demonstrates the most significant effect in this study. In contrast, effects below t-value limit are not likely to be significant. An effect is said to be positive when an increase in its level resulted in an increase in the response which coloured in orange while blue colour shows negative effect when increasing its level resulting response to be decrease.

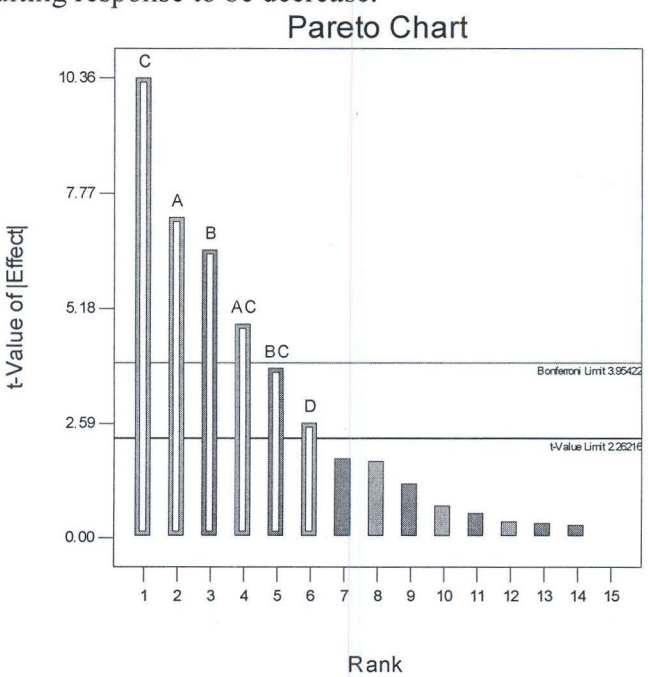

Figure 4: Pareto chart for t-value of effects

where A is time, B is initial glycerol concentration, C is initial H_2O_2 concentration and D is $CuFe_2O_4$ photocatalyst loadings.

Statistical Analysis and Analysis of Variance (ANOVA). The model equation of this study in coded factor is shown in Eq. (1) while the ANOVA analysis is summarized in Table 2. The

model with the selected terms was analyzed and found to be significant. The p-value was used as a tool to check the significance of each of the effects, which in turn may indicates the pattern of the interactions between the factors. The smaller the value of *p*, the more significant was the corresponding coefficient. P-value less than 0.05 indicate significant model terms and values greater than 0.05 indicate the model terms that are not significant.

Degradation (%) = 22.49 + 8.22*A – 7.39*B + 11.77*C + 2.96*D + 5.49*A*C -4.35*B*C (1)

where A is time, B is initial glycerol concentration, C is initial H_2O_2 concentration and D is $CuFe_2O_4$ photocatalyst loadings.

Table 2: ANOVA analysis of model

Source	Sum of Squares	df	Mean Square	F Value	p-value Prob > F	
Model	5094.099	6	849.0164	41.11545	< 0.0001	significant
A-time	1080.186	1	1080.186	52.31034	< 0.0001	
B-glycerol concentration	873.212	1	873.212	42.28717	0.0001	
C-H_2O_2 concentration	2215.186	1	2215.186	107.2752	< 0.0001	
D-$CuFe_2O_4$	140.0446	1	140.0446	6.781963	0.0285	
AC	482.2404	1	482.2404	23.35353	0.0009	
BC	303.2294	1	303.2294	14.68454	0.0040	
Residual	185.8461	9	20.64957			
Cor Total	5279.945	15				

The parameter such as the coefficient of determination (R^2), adjusted-R^2, predicted-R^2, coefficient of variance (CV), prediction residual error sum of squares (PRESS), adequate precision and the lack of fit test were used to determine the goodness of fit of a model. These parameter values can be taken from the ANOVA table. Table 3 summarizes the parameter used to test goodness of fit of the model.

Table 3: Parameter used to test goodness of fit of the model

Parameter	Value
Std. Dev.	4.54418
Mean	22.4858
CV %	20.20911
PRESS	587.3656
R-Squared	0.964801
Adj R-Squared	0.941336
Pred R-Squared	0.888755
Adeq Precision	20.18107

Coefficient of determination (R^2) is the proportion of variation in the response due to the model and it suggested that R^2 for a good model should be close to one. The R^2 of 0.965 was obtained

for the model, which is an indication of satisfactory result since the value is close to one. Addition of new variable to the model will affect the R^2 value. Therefore, adjusted R^2 is preferred to evaluate the model. To get a high degree correlation between actual and predicted values, the adjusted R^2 should be more than 90%. Adjusted R^2 of 94% was obtained for the model implying that all the selected terms that are significant were included and non-significance were left out.

The coefficient of variation (CV) is the standard deviation expressed as a percentage of the mean and is calculated by dividing the standard deviation by the mean value and multiplying by 100. Generally, CV value should be less than 10% for a good fit to the model. The CV of this model was 20.2% which is higher than 10%.

The amount of variation in new data explained by the model is measured by predicted-R^2. As a general rule, predicted-R^2 should be close to one for a good fit. Predicted-R^2 of 0.89 was obtained for this model.

Predicted Residual Error Sum of Squares (PRESS) value means an overall measurement of the discrepancy between the data and the estimation model. A good fit of the model should have smaller discrepancy. PRESS value 587.4 was obtained for this model.

The signal to noise ratio was measured by adequate precision test. A ratio greater than 4 is desirable. The adequate precision of this model is 20.181 indicates an adequate signal and this model can be used to navigate the design space.

Figure 5 shows the relationship between the predicted and experimental values for each response factor. The graph indicated that the predicted value were almost same as actual value.

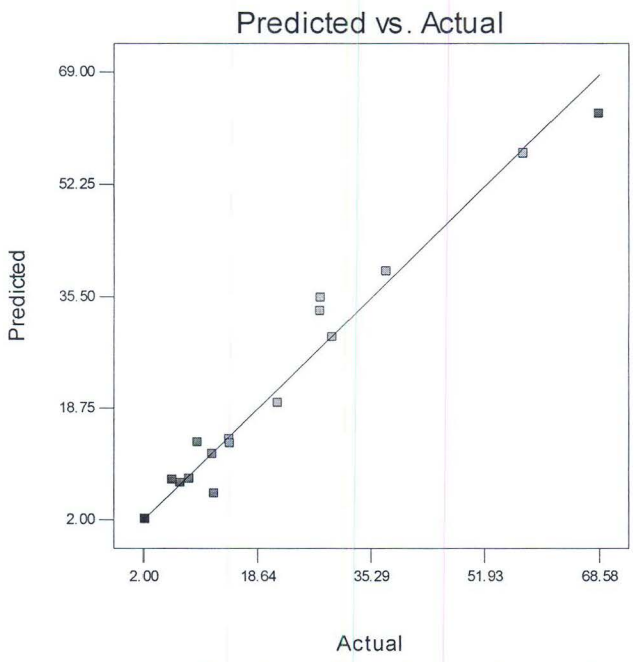

Figure 5: Comparison between predicted result and experimental result of factorial design

Response Surface of Glycerol Degradation. The interaction effects of factors upon the responses are depicted in the three-dimensional surface plots. Figure 6 shows the 3-D response surface plot of glycerol degradation at different function. The glycerol degraded faster as increasing the H_2O_2 concentration (Figure 6 (a)). Degradation of glycerol shows higher degradation values at 27.36 mM initial glycerol and 819.5 mM H_2O_2 (Figure 6 (b)).

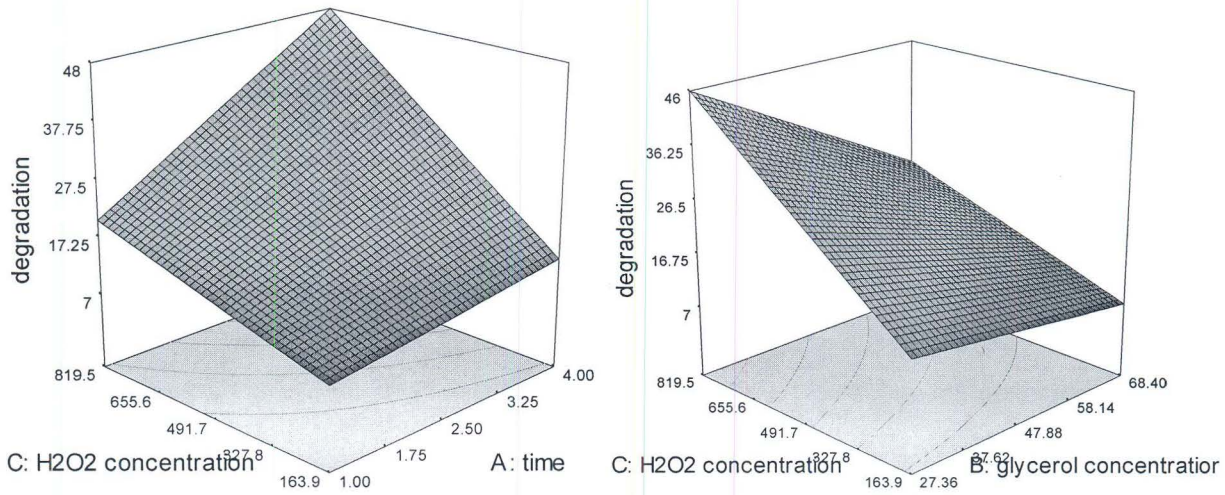

(a) (b)

Figure 6: Response surface plot of glycerol degradation as a function of: (a) different H_2O_2 concentration and time at fixed initial glycerol concentration and photocatalyst loading; (b) different initial glycerol concentration and H_2O_2 concentration at fixed time and photocatalyst loading

Prediction of Best Point. The verification of the experimental data was carried out by calculating numerically with the developed model where the objective was to degrade the initial glycerol concentration. The best experimental conditions for factors in glycerol degradation are shown in Table 4. The experiment was performed according to the suggested experimental conditions and the result was presented in Table 5. Based on the predicted and experimental results presented, the experimental values were in good agreement with the predicted values proposed by the model with error from 0.07% to 0.4%.

Table 4: Suggested best condition of factor in glycerol degradation

Factors	Best Condition
A-Time	4 h
B-Glycerol concentration	27.41 mM
C-H_2O_2 concentration	819.5 mM
D-$CuFe_2O_4$	5.0 g/L

Table 5: Comparison between predicted and experimental value for best condition

Response	Experimental Value	Error
Glycerol degradation	62.3	0.51%
	62.2	0.68%
	62.0	1.00%
Predicted value	62.62	
Desirability	0.910	

CONCLUSIONS

As a conclusion, $CuFe_2O_4$ photocatalyst prepared via sol-gel technique showed significant photocatalytic fenton activity towards the glycerol solution. In factorial analysis, H_2O_2 concentration showed larger significant effect as compared to the other factors such as photocatalyst loadings, glycerol concentration and time.

ACKNOWLEDGEMENT

Authors would like to thank the Ministry of Education, Malaysia for ERGS fund (RDU120613). Zi Ying Kong is thankful to Universiti Malaysia Pahang for providing GRS140333 scholarship throughout her studies.

REFERENCES

[1] Teske, S., Pregger, T., Simon, S., and Naegler, T. Energy evolution 2010—a sustainable world energy outlook. *Energy Efficiency*, Vol. 4, No. 3, 2011, pp. 409–433.

[2] Ediger, V. Ş., Hoşgör, E., Sürmeli, a. N., and Tatlıdil, H. Fossil fuel sustainability index: An application of resource management. *Energy Policy*, Vol. 35, No. 5, 2007, pp. 2969–2977.

[3] Savile, C., and Lalonde, J. Biotechnology for the acceleration of carbon dioxide capture and sequestration. *Current Opinion in Biotechnology*, Vol. 22, No. 6, 2011, pp. 818–823.

[4] Li, L., Du, W., Liu, D., Wang, L., and Li, Z. Lipase-catalyzed transesterification of rapeseed oils for biodiesel production with a novel organic solvent as the reaction. *Journal of Molecular Catalysis B: Enzymatic*, Vol. 43, 2006, pp. 58-62.

[5] Veljković, V. B., Stamenković, O. S., and Tasić, M. B. The wastewater treatment in the biodiesel production with alkali-catalyzed transesterification. *Renewable and Sustainable Energy Reviews*, Vol. 32, 2014, pp. 40–60.

[6] Yang, F., Hanna, M.A., Sun, R. Value-added uses for crude glycerol- a byproduct of biodiesel production. *Biotechnology for biofuels* Vol. 5, 2012, pp. 13.

[7] Gerpen, J.V. Biodiesel processing and production. *Fuel Processing Technology* Vol. 8, No. 10, 2005, pp. 1097-1107.

[8] Thompson J C, He B B. Characterization of crude glycerol from biodiesel production from multiple feedstocks. *Applied Engineering in Agriculture* Vol. 22, 2006, pp. 261-265.

[9] Wen, Z. New Uses for Crude Glycerin from Biodiesel Production, 2012. Retrieved on January 19, 2015 from http://www.extension.org/pages/29264/new-uses-for-crude-glycerin-from-biodiesel-production#.VLvMD9KUfkU\.

[10] Suehara, K., Kawamoto, Y., Fujii, E., Kohda, J., Nakano, Y., and Yano, T. Biological treatment of wastewater discharged from biodiesel fuel production plant with alkali-catalyzed

transesterification. *Journal of Bioscience and Bioengineering*, Vol. 100, No. 4, 2005, pp. 437–442.

[11] Li, M., Li, Y., Peng, S., Lu, G. and Li, S. Photocatalytic hydrogen generation using glycerol wastewater over Pt/TiO_2. *Front. Chem. China*, Vol. 4, No. 1, 2009, pp. 32-38.

[12] Slamet, Anny and Stiadi. Photocatalytic Hydrogen Generation from Glycerol and Water using Pt loaded N-doped TiO_2 Nanotube. *International Journal of Engineering & Technology* Vol. 11, 2011, pp. 3.

[13] Sadanandam, G., Lalitha, K., Kumari, V.D., Shankar, M.V. and Subrahmanyam, M. Cobalt doped TiO_2: A stable and efficient photocatalyst for continuous hydrogen production from glycerol: Water mixtures under solar light irradiation. *International journal of hydrogen energy*, Vol. 38, 2013, pp. 9655-9664.

[14] Liu, R., Yoshida, H., Fujita, S. and aria M. Photocatalytic hydrogen production from glycerol and water with NiO_x/TiO_2 catalysts. *Applied Catalysis B: Environmetal*, Vol. 144, 2014, pp. 41-45.

[15] Aazam, E. S. Photocatalytic oxidation of methylene blue dye under visible light by Ni doped Ag2S nanoparticles. *Journal of Industrial and Engineering Chemistry*, Vol. 20, No. 6, 2014, pp. 4033–4038.

[16] Casbeer, E., Sharma, V. K. and Li, X.-Z. Synthesis and photocatalytic activity of ferrites under visible light: A review. *Separation and Purification Technology*. Vol. 87, 2012, pp. 1-14.

[17] Shahid, M., Jingling, L., Ali, Z., Shakir, I., Warsi, M. F., Parveen, R. and Nadeem, M. Cobalt doped TiO_2: A stable and efficient photocatalyst for continuous hydrogen production from glycerol: Water mixtures under solar light irradiationPhotocatalytic degradation of methylene blue on magnetically separable $MgFe_2O_4$ under visible light irradiation. *Materials Chemistry and Physics*. Vol. 139, No. 2, 2013, pp. 566-571.

[18] Yang, H., Yan, J., Lu, Z., Cheng, X. and Tang, Y. Photocatalytic activity evaluation of tetragonal $CuFe_2O_4$ nanoparticles for the H_2 evolution under visible light irradiation. *Journal of Alloys and Compounds* Vol. 476, 2009, pp. 715-719.